9920 *Macromolecules* **2005,** *38,* 9920−9932

Poly(Phenylene-pyridyl) Dendrimers: Synthesis and Templating of Metal Nanoparticles

Zinaida B. Shifrina,*,† Marina S. Rajadurai,† Nina V. Firsova,† Lyudmila M. Bronstein,§ Xinlei Huang,§ Alexander L. Rusanov,† and Klaus Muellen*,‡

A. N. Nesmeyanov Institute of Organoelement Compounds, Russian Academy of Sciences, Vavilov St. 28, 119991 Moscow, Russia, Max Planck Institute for Polymer Research, Ackermannweg 10, 55128 Mainz, Germany, and Indiana University, Department of Chemistry, 800 E. Kirkwood Avenue, Bloomington, Indiana 47405

Received August 16, 2005; Revised Manuscript Received September 20, 2005

ABSTRACT: A new family of poly(phenylene-pyridyl) dendrimers (up to the fourth generation) with different periphery was synthesized via a divergent route by using a cascade of Diels−Alder cycloadditions. Tetra(4-ethynylphen-1-yl)methane served as a core. A new A_2B cyclopentadienone building block, namely, pyridine-containing cyclopentadienone with protected dienophile functions was prepared. By varying the building blocks at the last step of dendrimer construction, one could design molecules possessing either a phenyl- or a pyridyl-decorated outershell. The products were characterized by NMR spectroscopy, MALDI-TOF mass spectrometry, elemental analysis, atomic force microscopy, thermogravimetric analysis, DSC, and dynamic light scattering methods. These stiff polyphenylene dendrimers with pyridine embeds were then used as a matrix for encapsulation of Pd nanoparticles. The fourth-generation poly(phenylene-pyridyl) dendrimer with a phenyl-decorated periphery and pyridine-containing interior was found to serve as a powerful template for metal nanoparticle formation, resulting in excellent nanoparticle stability (no precipitation was observed for more than 6 months).

Introduction

Dendrimers are complex, but well-defined individual macromolecules with a high degree of order that can contain selected chemical units in predetermined sites of their structure.[1] Although some dendrimers have been synthesized more than twenty years ago,[2,3] the number of papers devoted to these monodisperse macromolecules of unique structure continues to increase. Dendrimers based on a diversity of repeat units were synthesized, including amides, amines, carbosilanes, siloxanes, esters, ethers, and various organometallic and amino acid-based structures.[4] With emphasis on aspects of application, dendrimers are currently studied as biomimetic catalysts,[5] building blocks for advanced materials,[6] drug delivery,[7] and as supports for catalysts.[8]

In contrast to dendrimers containing conformationally flexible single bonds, polyphenylene dendrimers are stiff, as conformational changes can only occur via rotation around the inter-ring C−C bonds.[9] Furthermore, these dendrimers possess high chemical and thermal stability[10] similar to linear polyphenylenes, but with greatly increased solubility due to the prevention of intermolecular packing, which is typical for linear poly-*p*-phenylenes. The first divergent synthesis of a polyphenylene dendrimer was described by ourselves[11,12] on the basis of repetitive Diels−Alder cycloaddition, while a convergent synthesis by Miller et al.[13] utilized transition-metal-catalyzed aryl−aryl coupling reactions. The cycloaddition approach is free of side reactions due to a noticeable shift of the reaction equilibrium toward the target products because of irreversible loss of CO followed by formation of an inner benzene ring. A key feature of the synthesis is that Diels−Alder cycloaddition is not influenced by the substituents of the tetraphenylcyclopentadienones as long as the latter survive the reaction temperatures.[12a,b] This allows incorporation of a variety of functional groups into dendrimers of the final generation by using disubstituted tetraphenylcyclopentadienones. These functional groups are exclusively located at the periphery of the dendrimers.

It is also worth noting that dendrimers have areas of different density, highly dense areas and voids,[14,15] so they can act as hosts for guest molecules. Moreover, because dendrimers have better-defined shape, size, and rigidity compared with polymers or surfactants, they have been proposed as well-defined “nanoreactors” and nanoporous stabilizers. Meijer pioneered the encapsulation of a guest into a “dendritic box” that was performed by the incorporation of the organic dye Bengal Rose into poly(propyleneimine) (PPI) dendrimers modified with amino acids.[16] Then, the molecular encapsulation strategy was developed for the formation of dendrimer-encapsulated metal nanoparticles.[17] Toward this end, flexible poly(amidoamine) (PAMAM) and PPI dendrimers were mainly used.[15,17,18] The relative rigidity of dendrimers hinders aggregation of their molecules onto metallic sites, and hence, the access to metallic catalytic sites is favored in dendrimers as compared with flexible polymers loaded by the same metal. From this point of view, stiff, shape persistent polyphenylene dendrimers are promising for preparation of highly active catalysts. In addition, high thermal stability of polyphenylene dendrimers opens up a possibility of carrying out otherwise impossible organic reactions with polymeric catalysts.

---

* Authors to whom correspondence should be addressed. E-mail: muellen@mpip-mainz.mpg.de (K.M.); shifrina@ineos.ac.ru (Z.S.).

† A. N. Nesmeyanov Institute of Organoelement Compounds.

‡ Max Planck Institute for Polymer Research.

§ Indiana University, Department of Chemistry.

10.1021/ma051802n CCC: $30.25

In this paper, we report the synthesis of new pyridine-containing polyphenylene dendrimers via the divergent route, starting from a tetrahedral core and appropriate cyclopentadienone branching reagents. Two types of dendrimers (up to the fourth generation) have been synthesized, one with a pyridine-functionalized periphery and one with pyridyl moieties arranged within the scaffold of the dendrimer molecule. The templating ability of third and fourth generation dendrimers has been studied for Pd nanoparticles.

Experimental Part

Materials. All starting materials were obtained from commercial suppliers (Aldrich, Fluka, Fischer, Acros, Riedel de Haen) and were used without purification. Solvents were used in HPLC grade purity as purchased. All atmosphere-sensitive reactions were performed under argon by using Schlenk techniques. Analytical thin-layer chromatography (TLC) was performed on commercial Merck plates coated with silica gel F-254.

Characterization. ^{1}H NMR spectra were recorded on a Bruker AMX 400 spectrometer. Chemical shifts were given in parts per million (ppm), using the solvent signal as a reference. Mass spectral analyses were carried out on ZAB2-SE-FPD (VG Analytical) and Bruker Reflex-TOF spectrometers. MALDI-TOF mass spectra were measured by using a 337 nm nitrogen laser and 1,8,9-trihydroxyanthracene as a matrix. Thermogravimetry analysis measurements (TGA) were carried out on a Mettler TG50 instrument in air. Differential scanning calorimetry (DSC) was performed on a Mettler DSC instrument at 10°/min. Absorption spectra were recorded on a UVIKON 931 UV−vis spectrometer (Kontron, USA) in the wavelength range of 200−700 nm. The optical path length was 0.1 cm, and THF was used as a reference for all measurements.

Transmission electron microscopy (TEM) measurements were carried out with a JEOL JEM1010 instrument at an electron accelerating voltage of 60 kV. A drop of the diluted sample in chloroform (0.75 mg/mL) was placed on a carbon-coated copper grid situated on absorbent paper and allowed to dry in open air for 1 day.

Atomic force microscopy (AFM) experiments were performed in tapping mode by using the Nanoscope IIIa (Digital instruments, USA) multimode scanning probe microscope. Commercially available standard silicon 125 μm tapping mode cantilevers (Nanoprobe) were used. The resonant frequency was in the interval 300−350 kHz, the scan rate was maintained at 1.5−2.0 Hz. The samples (1×10^{-7} mol/L solutions of G3 and G4 in chloroform) were applied onto a freshly cleaved mica surface and allowed to dry in air at room temperature.

X-ray diffraction (XRD) experiments were performed by using a Rigaku D/max-Rc diffractometer with a 12 kW X-ray radiation source. The $K_{\alpha 1}$ line of a copper-anode radiation was used. The primary radiation was monochromatized by a tunable double-reflection silicon crystal monochromator.

The Malvern Instruments Zetasizer Nano-6 dynamic light scattering (DLS) instrument was used to determine dendrimer sizes in chloroform solutions before and after metalation. DLS experiments were carried out at a 90° scattering angle and 25 °C.

Elemental analysis on Pd was carried out by using X-ray fluorescence measurements performed with a Zeiss Jena VRA-30 spectrometer equipped with a Mo anode, a LiF crystal analyzer, and a SZ detector. Analyses were based on the Co K_α line, and a series of standards were prepared by mixing 1 g of polystyrene with 10−20 mg of standard compounds. The time of data acquisition was held constant at 10 s.

Synthesis of Tetrakis(4-ethynylphen-1-yl)methane (Td). Tetrakis(4-ethynylphen-1-yl)methane was synthesized as described elsewhere.[19]

Synthesis of 1,3-Di-pyridin-2-yl-propan-2-one (4). 2-Picoline (60 mL, 0.56 mol) was slowly added to freshly prepared phenyllithium (53.4 g, 0.63 mol) in diethyl ether (500 mL) and refluxed for 30 min. 2-Pyridylacetonitrile (25 g, 0.21 mol) was added dropwise to the mixture and refluxed for 1.5 h. After cooling, the reaction product was poured into aqueous 2N hydrochloric acid. The aqueous layer was separated, refluxed for 1.5 h, neutralized, and then extracted with chloroform. The chloroform extract was dried over magnesium sulfate, and the solvent was removed under reduced pressure. The residual oil was fractionated to give 45% (20.2 g) of 1,3-di-pyridin-2-yl-propan-2-one, bp 130−135 °C/5 mm Hg, mp 80−81 °C. ^{1}H NMR spectrum (400 MHz, DMSO-d_6): 5.44 (CH-enol form, s), 3.68 (CH$_2$-enol form, s), 4.07 (CH$_2$-ketone form, s), 8.48, 8.25, 7.34 (3d, 4H, PyH) 7.65−7.76, 7.29−7.21, 7.08−6.90 (3m, 12H, PyH). Elem anal. calcd for $C_{13}H_{12}N_2O$, %: C, 73.57; H, 5.70; N, 13.20; found: C, 73.55; H, 5.73; N, 13.18.

4,4′-Bis(triisopropylsilylethynyl)benzyl (3). 4,4′-Bis(triisopropylsilylethynyl)benzyl was synthesized from 4,4′-dibromobenzyl via Pd-catalyzed coupling with triisopropylsilylacetylene (TiPSA) as described elsewhere.[10]

Synthesis of 3,4-Bis-(4-(triisopropylsilylethynyl)-phen-1-yl)-2,5-dipyrid-2-yl-cyclopentan-2,4-dienone (1). 4,4′-Bis(triisopropylsilylethynyl) benzyl (**3**) (4 g, 7 mmol) and dipyridylacetone (**4**) (1.49 g, 7 mmol) was dissolved in 17 mL of ethanol, and the resulting solution was heated at 60 °C and stirred for 5 min under argon atmosphere. Then a solution of KOH (0.02 g, 0.36 mmol) in 5 mL of ethanol was added slowly. The reaction was carried out for 0.5 h and controlled by TLC (80% hexane/20% CH$_2$Cl$_2$). After cooling, about 5 mL of ethanol was added, and the reaction mixture was kept overnight without stirring.

The product precipitated (enolone) was filtered, dried, and put into ethylene glycol, where cyclization to cyclopentadienone was performed at 200 °C for 0.5 h. Cyclization also can occur in situ in a further Diels−Alder reaction. The product was received as orange crystals with yield of 78% (3.88 g), mp 166−167 °C. ^{1}H NMR spectrum (400 MHz, CDCl$_3$): 8.70 (d, 1 H, PyH), 8.55 (d, 1 H, PyH), 7.73 (t, 1 H, PyH), 7.62 (t, 1 H, PyH), 7.44−7.15 (m, ArH), 1.09 (s, 42H, aliph). FD-MS: *m/z* (u e^{-1}): 746.7 (M$^+$). Elem anal. calcd for $C_{49}H_{58}N_2OSi_2$, %: C, 78.77; H, 7.82; N, 3.75; found: C, 78.50; H, 7.93; N, 3.80.

Synthesis of 2,3,4,5-Tetrapyrid-2-yl-cyclopenta-2,4-dienone (2). 1,2-Di-pyridin-2-yl-ethane-1,2-dione (2 g, 9.42 mmol) and 1,3-di-pyridin-2-yl-propan-2-one (1.99 g, 9.42 mmol) were dissolved in ethanol (14 mL) at 60 °C under Ar. A solution of KOH (0.03 g, 0.54 mmol) in ethanol (1.5 mL) was added slowly for 2−3 min. The reaction was carried out for 0.5 h and was controlled by TLC. The solvent was removed by rotary evaporation, and the orange powder was recrystallized from diethyl ether with a yield of 74% (2.71 g). Enolone formed was transferred into cyclopentadienone via the above procedure. ^{1}H NMR spectrum (400 MHz, CDCl$_3$): 8.69, 8.66 (2d, 2H, PyH), 8.50, 8.43 (2d, 2H, PyH), 7.85−7.69 (m, 4H, PyH), 7.66−6.93 (m, 8H, PyH). FD-MS: *m/z* (u e^{-1}): 388 (M$^+$). Elem anal. calcd for $C_{25}H_{16}N_4O$, %: C, 77.31; H, 4.15; N, 14.42; found: C, 77.51; H, 4.23; N, 14.06.

General Procedure for the Diels−Alder Reaction Between Tetraarylcyclopentadienones and Aryl-ethynyl Derivatives. The reaction was carried out in a Schlenk flask under argon. The reaction flask with the cyclopentadienone (Cp, 1.5−2 mol of Cp per 1 ethynyl group) solution in *o*-xylene (or diphenyl ether for high generations) (4.5×10^{-3} mol/L) was evacuated and filled with argon three times and then heated to 100 °C. A solution of aryl-ethynyl derivative in *o*-xylene was slowly added, the temperature was increased up to reflux. The reaction was controlled by TLC, and the reaction time was dependent on the generation and varied from 5 h for G1 and G2 to 45 h for G4. After cooling, the solvent was evaporated, a small amount of CH_2Cl_2 was added, and the compound was precipitated in methanol.

General Procedure for the Desilylation of Triisopropylsilyl (TiPS) Substituted Dendrimers. Triisopropylsilyl-substituted dendrimer (0.06 mmol) was dissolved in a mixture of THF (20 mL) and benzene (6 mL). To this solution, tetrabutylammonium fluoride trihydrate (3 mol Bu_4NF per 1 triisopropylsilyl group) in THF (6 mL) was added. After 8 h stirring, CH_2Cl_2 (5 mL) was added, and the organic phase was washed with water and dried over $MgSO_4$. After evaporating the solvent, the crude product was purified by reprecipitation in methanol.

Synthesis of Td-G1-(EthynylTiPS)$_8$. This compound was prepared according to a general procedure (see above) for the Diels−Alder reaction between tetraarylcyclopentadienones and aryl-ethynyl derivatives by using tetra(4-ethynylphen-1-yl)methane (**Td**) (0.416 g, 1 mmol) and 3,4-bis-(4-(triisopropylsilylethynyl)phen-1-yl)-2,5-dipyrid-2-yl-cyclopentan-2,4-dienone (**1**) (4.4831 g, 6 mmol). Yield: 91% (1.35 g). ^{1}H NMR spectrum (400 MHz, CDCl$_3$): 8.58 (d, 4H, PyH), 8.25 (d, 4H, PyH), 7.78 (s, 4H, ArH), 7.49−6.52 (m, 72H, ArH), 1.09(s, 42H, aliph). MALDI-TOF *m/e*: 3293 (M$^+$, calcd 3293.26). Elem anal. calcd for $C_{225}H_{252}N_8Si_8$, %: C 82.0, H 7.71, N 3.40, Si 6.82; found: C 80.99, H 7.39, N 3.10, Si 6.51.

Synthesis of Td-G1-(Ethynyl)$_8$ (5). A solution of 1.35 g (0.41 mmol) of **Td-G1-(EthynylTiPS)$_8$** in THF (170 mL) and benzene (50 mL) was treated according to the general procedure (see above) for desilylation of triisopropylsilyl derivatives. Yield: 83.8% (0.7 g). ^{1}H NMR spectrum (400 MHz, CDCl$_3$): 8.58 (d, 4H, PyH), 8.24 (d, 4H, PyH), 7.81 (s, 4H, ArH), 7.45−6.55 (m, 72H, ArH), 3.01, 2.97 (2s, 8H, acetylenes). FD-MS: *m/z* (u e^{-1}): 2042 (M$^+$, calcd 2042.49). Elem anal. calcd for $C_{153}H_{92}N_8$, %: C 89.97, H 4.54, N 5.49; found: C 88.82, H 4.37, N 5.31.

Synthesis of Td-G2-(EthynylTiPS)$_{16}$. This compound was prepared according to the general procedure (see above) for the Diels−Alder reaction between tetraarylcyclopentadienones and aryl-ethynyl derivatives by using **Td-G1-(Ethynyl)$_8$** (**5**) and 3,4-bis-(4-(triisopropylsilylethynyl)phen-1-yl)-2,5-dipyrid-2-yl-cyclopentan-2,4-dienone (**1**). Yield: 62.8%. ^{1}H NMR spectrum (400 MHz, CDCl$_3$): 8.62 (d, 12H, PyH), 8.30 (d, 12H, PyH), 7.78, 7.74, 7.68 (3s, 12H, ArH), 7.48−6.51 (m, 184H, ArH), 1.09(s, 336H, aliph). MALDI-TOF *m/e*: 7820 (M $^+$ Na, calcd 7795.96). Elem anal. calcd for $C_{537}H_{556}N_{24}Si_{16}$, %: C 82.74, H 7.19, N 4.31, Si 5.76; found: C 81.79, H 6.92, N 4.22, Si 5.48.

Synthesis of Td-G2-(Ethynyl)$_{16}$. A solution of **Td-G2-(EthynylTiPS)$_{16}$** in THF and benzene was treated according to the general procedure (see above) for the desilylation of triisopropylsilyl derivatives. Yield: 68.3%. ^{1}H NMR spectrum (400 MHz, CDCl$_3$): 8.62 (d, 12H, PyH), 8.28 (d, 12H, PyH), 7.78, 7.77, 7.72 (3s, 12H, ArH), 7.47−6.52 (m, 184H, ArH), 3.05, 3.02 (2s, 16H, acetylene). MALDI-TOF *m/e*: 5293 (M$^+$, calcd 5294.42). Elem anal. calcd for $C_{393}H_{236}N_{24}$, %: C 89.16, H 4.49, N 6.35; found: C 88.06, H 4.31, N 6.22.

Synthesis of Td-G3-Ph (7). This compound was prepared according to the general procedure (see above) for the Diels−Alder reaction between tetraarylcyclopentadienones and aryl-ethynyl derivatives by using **Td-G2-(Ethynyl)$_{16}$** and 2,3,4,5-tetraphenylcyclopentadienone. Yield: 74%. ^{1}H NMR spectrum (400 MHz, CDCl$_3$): 8.54 (d, 12H, PyH), 8.18 (d, 12H, PyH), 7.73−7.62 (m, 28H, ArH), 7.50−6.39 (m, 504H, ArH). MALDI-TOF *m/e*: 10995 (M$^+$, calcd 10997.97). Elem anal. calcd for $C_{841}H_{556}N_{24}$, %: C 91.85, H 5.10, N 3.06; found: C 90.68, H 4.88, N 2,91.

Synthesis of Td-G3-Py (8). This compound was prepared according to the general procedure (see above) for the Diels−Alder reaction between tetraarylcyclopentadienones and aryl-ethynyl derivatives by using **Td-G2-(Ethynyl)$_{16}$** and 2,3,4,5-tetrapyridylcyclopentadienone (**2**). Yield: 71%. MALDI-TOF *m/e*: 11061.60 (M$^+$, calcd 11061.17). Elem anal. calcd for $C_{777}H_{492}N_{88}$, %: C 84.37, H 4.48, N 11.14; found: C 83.27, H 4.31, N 10.96.

Synthesis of Td-G3-(EthynylTiPS)$_{32}$. This compound was prepared according to the general procedure (see above) for the Diels−Alder reaction between tetraarylcyclopentadienones and aryl-ethynyl derivatives by using **Td-G2-(Ethynyl)$_{16}$** and 3,4-bis-(4-(triisopropylsilylethynyl)phen-1-yl)-2,5-dipyrid-2-yl-cyclopentan-2,4-dienone. The reaction was carried out in diphenyl ether at 200 °C for 72 h. Yield: 65%. ^{1}H NMR spectrum (400 MHz, CDCl$_3$): 8.55 (d, 28H, PyH), 8.24 (d, 28H, PyH), 7.68, 7.62, 7.59 (3s, 28H, ArH), 7.42−6.30 (m, 408H, ArH), 1.09 (s, 672H, aliph). MALDI-TOF *m/e*: 16804 (M$^+$, calcd 16801.35). Elem anal. calcd for $C_{1161}H_{1164}N_{56}Si_{32}$, %: C 83.00, H 6.98, N 4.67, Si 5.35; found: C 81.82, H 6.66, N 4.39, Si 5.11.

Synthesis of Td-G3-(Ethynyl)$_{32}$ (6). A solution of **Td-G3-(EthynylTiPS)$_{32}$** in THF and benzene was treated according to the general procedure (see above) for the desilylation of triisopropylsilyl derivatives. Yield: 80%. ^{1}H NMR spectrum (400 MHz, CDCl$_3$): 8.53 (d, 28H, PyH), 8.21 (d, 28H, PyH), 7.69, 7.64, 7.57 (3s, 28H, ArH), 7.42−6.30 (m, 408H, ArH), 2.99−2.95 (m, 32H, acetylenes). MALDI-TOF *m/e*: 11796 (M $^+$, calcd 11798.29). Elem anal. calcd for $C_{873}H_{524}N_{56}$, %: C 88.88, H 4.48, N 6.65; found: C 88.00, H 4.32, N 6.44.

Synthesis of Td-G4-Ph (9). This compound was prepared according to the general procedure (see above) for the Diels−Alder reaction between tetraarylcyclopentadienones and aryl-ethynyl derivatives by using **Td-G3-(Ethynyl)$_{32}$** and 2,3,4,5-tetraphenylcyclopentadienone. The reaction was carried out in diphenyl ether at 200 °C for 120 h. Yield: 77%. ^{1}H NMR spectrum (400 MHz, CDCl$_3$) 8.52 (d, 28H, PyH), 8.18 (d, 28H, PyH), 7.71−7.53 (m, 60H, ArH), 7.49−6.30 (m, 1048H, ArH). MALDI-TOF *m/e*: 23 283.2 (M$^+$ + 2K$^+$), calcd 23205.38

Scheme 1. General Scheme of Synthesis of Pyridine-Containing Polyphenylene Dendrimers

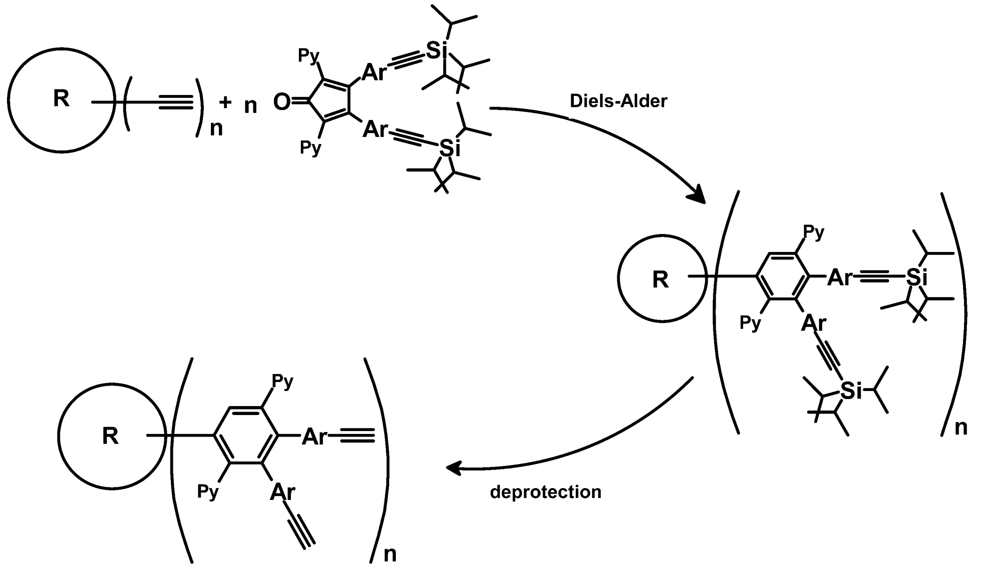

(M^+). Elem anal. calcd for $C_{1769}H_{1164}N_{56}$, %: C 91.56, H 5.06, N 3.38; found: C 90.49, H 4.91, N 3.29.

General Procedure for the Preparation of Dendrimer-Encapsulated Metal Nanoparticles. The reaction was carried out in a Schlenk flask under argon. To the dendrimer solution (4.5×10^{-5} mol/L) in THF was slowly added the THF solution of $Pd(CH_3COO)_2$ (1 mol of Pd(II) per 2 pyridine fragments). After 8 h of stirring, the reaction solution was evacuated, filled with argon three times, and then triethylsilane was added (2 mol of triethylsilane/Pd(II)) under argon atmosphere. The light-yellow dendrimer/$Pd(CH_3COO)_2$ solution immediately turned brown or dark brown, indicating the Pd(0) nanoparticle formation.

Preparation of Td-G3-Ph/Pd(0). The solution was prepared according to the general procedure (see above) by using **Td-G3-Ph** (**7**) (0.050 g, 4.5×10^{-6} mol) and $Pd(CH_3COO)_2$ (0.012 g, 5.4×10^{-5} mol) in THF (100 mL). Elem anal. calcd for $C_{841}H_{556}N_{24} + 12Pd(CH_3COO)_2$: Pd, 9.33%; found: Pd, 9.08%.

Preparation of Td-G4-Ph/Pd(0). The solution was prepared according to the general procedure (see above) by using **Td-G4-Ph** (**9**) (0.061 g, 2.7×10^{-6} mol) and $Pd(CH_3COO)_2$ (0.017 g, 7.6×10^{-5} mol) in THF (60 mL). Elem anal. calcd for $C_{1769}H_{1164}N_{56} + 28Pd(CH_3COO)_2$: Pd, 10.11%; found: 9.00%.

Results and Discussion

Synthesis of Building Blocks. The synthesis of pyridine-containing dendrimers was based on two reactions: the Diels−Alder cycloaddition of tetrasubstituted cyclopentadienones to ethynes and the deprotection of triisopropylsilyl (TiPS) substituted alkynes (Scheme 1).

Toward this end, we have introduced here the A_2B building block **1**. In addition, we have synthesized tetrapyrid-2-yl-cyclopentadienone **2** without the ethynyl-TiPS substituents for the final cycloaddition step to generate a fully pyridine-loaded periphery.

The syntheses of tetrasubstituted cyclopentadienones were performed by Knoevenagel condensation according to Scheme 2.

The reaction of 4,4′-bis(triisopropylsilylethynyl)benzyl (**3**) and 1,3-dipyrid-2-yl-2-propanone (**4**) with KOH in ethanol resulted in a product with a surprisingly orange color instead of dark purple, which is typical for cyclopentadienones. We have found that, at standard Knoevenagel conditions, the cyclopentadienone is not formed. Instead, the reaction leads to enolone **1′** (Scheme 2). Only the reaction of the enolone with ethylene glycol at 200 °C led to the target product **1**. The synthesis of cyclopentadienone **2** was performed from commercially available 2,2′-pyridyl and 1,3-dipyrid-2-yl-2-propanone (**4**). In both cases, the Knoevenagel condensation afforded yields of around 80%. The synthesis of 1,3-dipyrid-2-yl-2-propanone (**4**) was carried out via addition of picolyllithium to 2-pyridylacetonitrile. According to the ^1H NMR spectrum, **4** gave rise to an enol−ketone equilibrium. Further, under Knoevenagel conditions (i.e., in the presence of catalytic amount of KOH), equilibrium was shifting to the ketone form, providing the successful accomplishment of the reaction and formation of the cyclopentadienones.

The characterization of the obtained cyclopentadienones was performed by using ^1H NMR spectroscopy, field desorption (FD) mass spectrometry, and elemental analysis. The data obtained confirmed the purity of the compounds (see Experimental Section).

The synthesis of 1,2-bis-(5-bromo-pyrid-2-yl)ethan-1,2-dione (**3′**) based on monolithiation of 2,5-dibromopyridine, followed by condensation with 1,4-dimethylpiperazine-2,3-dione, was carried out according to Scheme 3. The concentration was found to play a significant role in the selectivity of lithiation. The more dilute the solution, the higher is the preference for the 2-position. Under such reaction conditions, 5-bromo-2-lithiopyridine is both kinetically and thermodynamically favored.[20] Then the compound obtained was allowed to react with 1,4-dimethylpiperazine-2,3-dione to yield, after hydrolysis, 1,2-bis(5-bromo-pyrid-2-yl)ethan-1,2-dione (**3′**). However, the yield of the ketone did not exceed 22%, and the product obtained was unstable, so no further experiments were carried out with this compound.

Synthesis of Dendrimers. Synthesis of dendrimers by the divergent method started with the Diels−Alder cycloaddition of building unit **1** to tetra(4-ethynylphenyl)methane (**Td**)[19] (Scheme 4). Subsequent cleavage of the TiPS groups yielded the corresponding ethynyl-substituted first-generation dendrimer **Td-G1-(Ethynyl)$_8$** (**5**). A repetitive sequence of the cycloaddition and

Scheme 2. Synthesis of the Building Blocks[a]

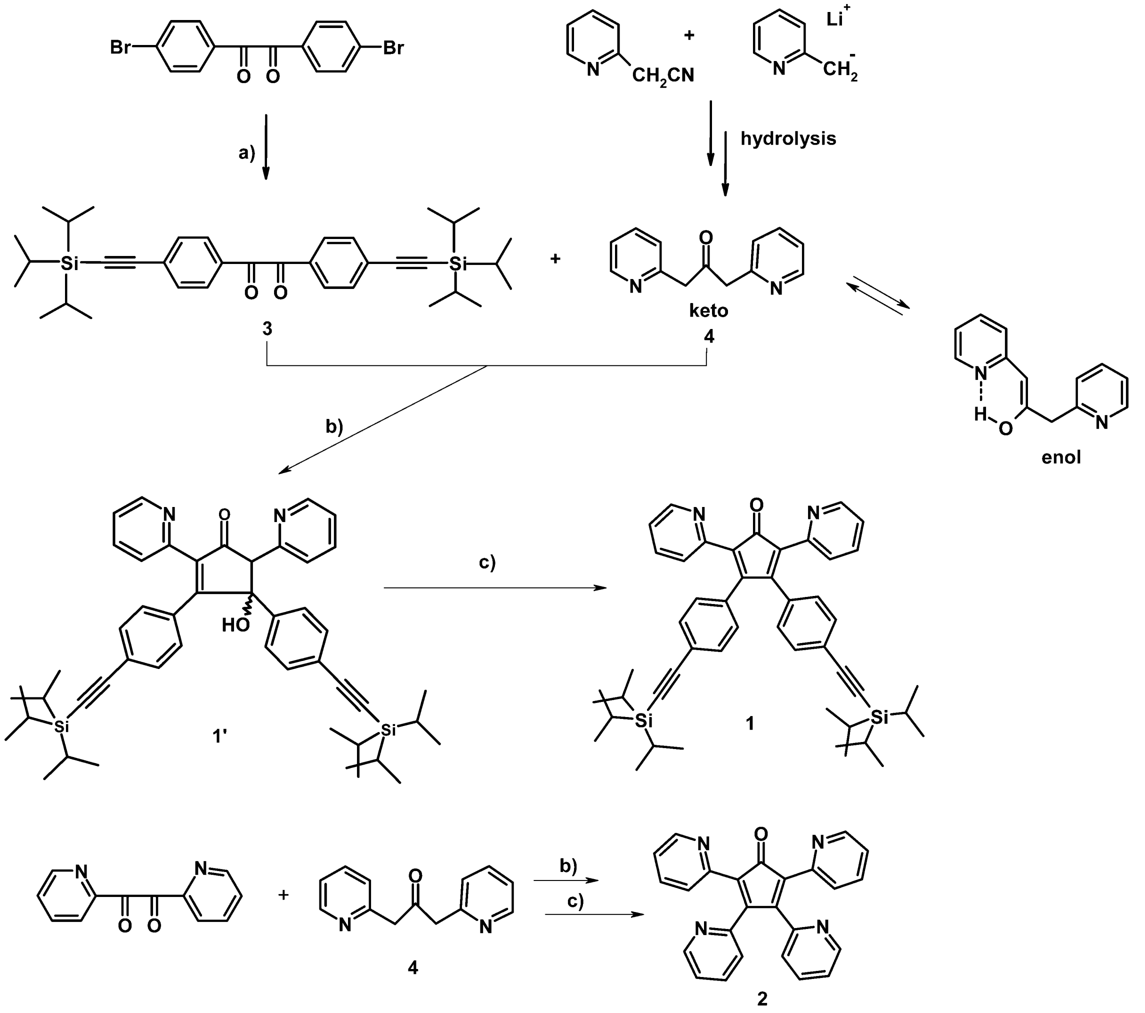

[a] Key: (a) triisopropylsilylacetylene, $Pd(PPh_3)_2Cl_2$, CuI, PPh_3, Et_3N/toluene; (b) KOH, C_2H_5OH, 60 °C; (c) ethylene glycol, 200 °C.

Scheme 3. Synthesis of 4,4-Dibromo-2,2-pyridyl

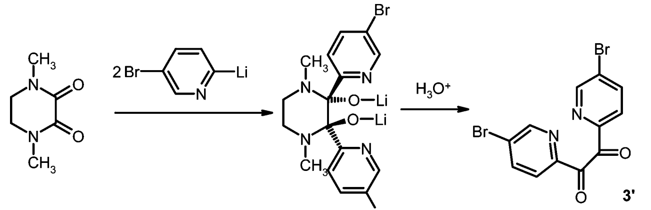

unstable compound, poor yield

the deprotection steps allowed the construction of the succeeding generations of dendrimers. Using the above protocol, dendrimers up to the fourth generation have been synthesized. By varying the building blocks at the final cycloaddition step, differently functionalized peripheries of the dendrimers could be achieved. Using **1,** parent tetraphenylcyclopentadienone, and **2**, **Td-G3-(Ethynyl)$_{32}$** (**6**), **Td-G3-Ph** (**7**), and **Td-G3-Py** (**8**) have been obtained, respectively (Scheme 4). By adding the parent tetraphenylcyclopentadienone to ethynyl-substituted (**6**), the **Td-G4-Ph** (**9**) with a phenyl-decorated periphery was prepared. As the substituents of the building block did not influence the cycloaddition itself, reactions with participation of different building blocks could be carried out under the same conditions. As was revealed for the parent polyphenylene dendrimers,[10] solvent reflux increases the rate of cycloaddition, assisting the elimination of carbon monoxide at temperatures above 130 °C under inert atmosphere. It appears that these conditions are also appropriate for Diels−Alder cycloaddition of pyridine-containing derivatives, so these reactions were carried out in *o*-xylene at reflux. For isolation of the dendrimers, repeated precipitations in ethanol (for high generations in a hexane/pentane mixture) were used, followed by MALDI-TOF mass spectrometry, which proved the absence of side products resulting from incomplete Diels−Alder cycloadditions. The deprotection of the TiPS-ethyne-substituted dendrimers was performed by using ammonium fluoride and catalytic amounts of tetrabutylammonium fluoride in tetrahydrofuran (THF) and did not require any purification.

Unfortunately, we were unable to synthesize **Td-G4-(EthynylTiPS)$_{64}$** (**10**). While the deprotection of **Td-G3-(EthynylTiPS)$_{32}$** gave pure **Td-G3-(Ethynyl)$_{32}$** (**6**), a further Diels−Alder cycloaddition with cyclopentadienone **1** failed to furnish a pure product. We believe that this is caused by strong crowding in the outer shell of the high generations of dendrimers. We assumed that, if there is enough space to add 32 unsubstituted cyclopentadienones under formation of **Td-G4-Ph** (**9**), then the room is insufficient to accommodate 32 A_2B building blocks carrying additional TiPS-ethynyl groups.

Physical Properties and Characterization. The dendrimers prepared are soluble in a wide range of

Scheme 4. Divergent Synthesis of Polyphenylene Dendrimers with Pyridine Embeds[a]

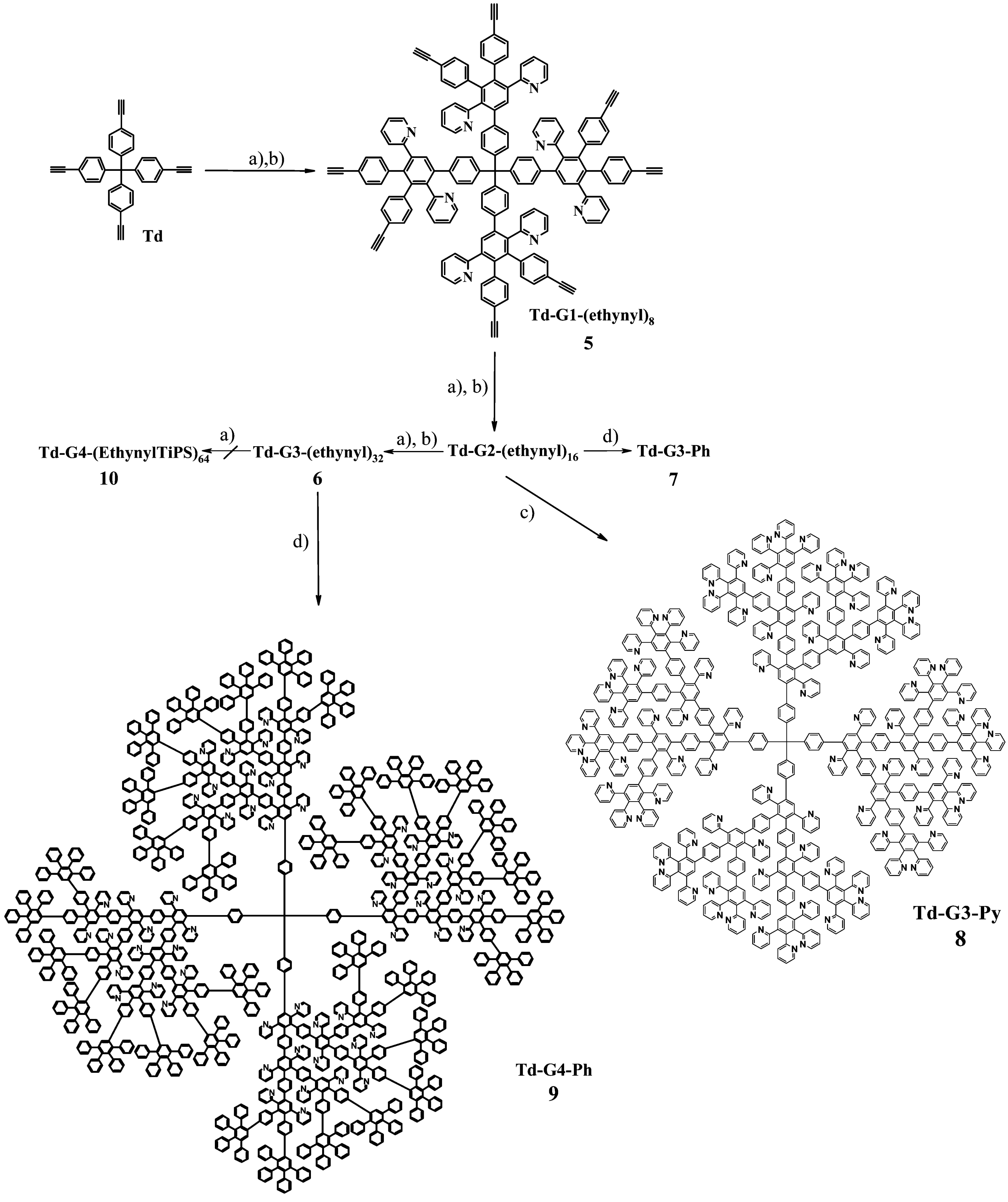

[a] Key: (a) **1**, *o*-xylene, reflux; (b) NH_4F, Bu_4NF, THF, r.t.; (c) **2**, *o*-xylene, reflux; (d) tetraphenylcyclopentadienone, diphenyl ether, 200 °C.

solvents, but the solubility depends on the dendrimer structure. While the pyridine-containing dendrimers with phenyl-decorated periphery are soluble in chlorinated solvents, THF, toluene and, no matter what the generation is, could thus be isolated by precipitation into ethanol or hexane, starting from the second-generation TiPS-ethynyl-substituted dendrimers and dendrimers with a pyridine-functionalized periphery **6**, **8** were found to be soluble in ethanol and other aliphatic alcohols except methanol.

For a characterization of dendrimers, ^1H NMR spectroscopy and MALDI-TOF mass spectrometry were applied. For all dendrimers, ^{1}H NMR signals of protons at the central ring of pentaphenyl-substituted benzene units could be detected clearly for each generation layer as well as the signals of α-protons of the pyridine units, which are shifted toward low field. The spectrum of **G1** (Figure 1a) shows singlet at $\delta = 7.82$ ppm assigned to four equivalent protons of the pentasubstituted benzene units, and two signals at $\delta = 8.58$ and 8.24 ppm attributed to α-protons of nonequivalent pyridine moieties. The ^{1}H NMR spectra of **G2** and **G3** (Figure 1b,c) show doublets between $\delta = 8.6$ and 8.1 ppm, ascribed to α-protons of pyridines located at the first and next layers of a dendrimer and a singlet of protons of the pentasubstituted aromatic units at $\delta = 7.66-7.80$ ppm.

More detailed information on the structure of the dendrimers could not be achieved from ^{1}H NMR spectra because of the strong overlap of signals in an aromatic region. Conversely, for ethynyl- and TiPS-ethynyl-substituted dendrimers, the ratio between aliphatic and aromatic protons correlates well with the expected structure.

By using MALDI-TOF mass spectrometry, we were able to determine the molecular mass of dendrimers and to confirm that the dendrimers are monodisperse. Any defects coming from incomplete Diels–Alder cycloaddition in the dendrimer synthesis would result in a mass difference of 719 or a multiple of that (mass of cyclone unit minus CO) and would easily be detectable by this method. Figure 2 represents the MALDI-TOF mass spectrum of **Td-G4-Ph** (**9**) recorded in the presence of potassium salt. The molecular peak at 23 283 g/mol (mass of molecule + mass of two potassium cations) is in good agreement with the mass calculated for $C_{1769}H_{1164}N_{56}$ 2 K (23 283.6 g/mol). Furthermore, the signal is accompanied by the molecular peak at 23 204 g/mol with low intensity corresponding to **Td-G4-Ph** without salt. Molecular masses of the dendrimers of second and third generations determined by MALDI-TOF mass spectrometry also matched the calculated values.

According to thermogravimetric analysis (TGA), the dendrimers show the thermal stability typical for polyphenylene structures.[21] Degradation (10% weight loss) starts at 575 °C under nitrogen and at 480 °C under air. The DSC traces of all the dendrimers did not show any phase changes up to the decomposition temperature. High conformational and thermal stability of these dendrimers make them unique among all other dendrimers containing pyridine or amine (imine) functional groups.

Figure 3 shows the AFM images of **7** and **9** absorbed on freshly cleaved mica by spin-coating of 1×10^{-7} M chloroform solutions.

The dendrimer sizes for **7** and **9** were determined by using height estimation of the particles. The values acquired are 5.5 nm for (**7**) and 6.7 nm for (**9**) (Figure 4). The uniformity of the observed spots and the relatively narrow height distribution lead us to believe that only individual dendrimers are present on the mica surface and that aggregation has not occurred. The values gained reasonably agree with dendrimer diameter calculations carried out by using models obtained with molecular mechanics and dynamics approaches (Cerius 2 molecular modeling package) for parent phenylene dendrimers.[9,10]

Nanoparticle Formation. Coordination between metal compounds and donor groups leads to metal incorporation inside various polymer particles, such as block copolymer micelles[22,23] or dendrimers studied by Tomalia,[15] Crooks,[17] and Gröhn.[18]

We anticipated that, for dendrimers decorated with peripheral pyridine groups, interaction with metal compounds would result in precipitation of the composite material from solution due to intermolecular cross-linking with metal compounds.[24] On the other hand, the dendrimers with a pyridine-functionalized interior and phenyl periphery should retain their solubility after incorporation of metal compounds due to intramolecular complexation.[25] The polyphenylene periphery in this case should prevent cross-linking and precipitation. As can be seen from the space filling model[26] presented in Figure 5 for **9**, this dendrimer also contains voids (or areas with loose filling), facilitating the accommodation of nanoparticles. Thus, after metal reduction, the metal nanoparticles stabilized within dendrimer voids by steric interaction, and specific adsorption of pyridine groups with a nanoparticle surface[27] should be formed. Steric crowding on the periphery should prevent the release of metal nanoparticles from dendrimers.

Nanoparticle characteristics and morphology depend on a number of factors, which will be considered in the following discussion. For encapsulation of metal in dendrimers with phenyl-decorated periphery, we used $Pd(CH_3COO)_2$. This choice was dictated by the good solubility of this salt as well as of dendrimers in the common organic solvents such as THF. As was expected, interaction of the peripherally pyridine-decorated dendrimer **8** with $Pd(CH_3COO)_2$ resulted in immediate precipitation of the complex due to intermolecular coordination with the Pd salt; therefore, the following discussion considers only phenyl-decorated dendrimers. We studied the influence of metal compound loading, dendrimer concentration, reduction rate, and dendrimer generation on the Pd nanoparticle size. The majority of the experiments have been performed with **Td-G4-Ph** (**9**), while **Td-G3-Ph** (**7**) was only used to compare the two generations of the dendrimers.

The maximum amount of the Pd salt loaded into the dendrimers is defined by the number of pyridine ligands in a dendrimer. We assumed that Pd(II) coordinates two pyridine fragments of a dendrimer.[28] Therefore, at a molar ratio N:Pd of 2:1, 12 $Pd(CH_3COOH)_2$ molecules can be absorbed by **Td-G3-Ph** and 28 molecules by **Td-G4-Ph**. Elemental analysis (see Experimental Section) on the Pd content performed after incorporation of Pd salt confirmed this assumption. Moreover, attempts to incorporate more Pd salt into dendrimers (at a molar ratio of N:Pd of 1:1) led to the same Pd content in the final product and to presence of the salt in the filtrate after isolation of the dendrimer–salt complex.

The concentration of dendrimers in the reaction solution significantly affects metalation. At high dendrimer concentrations (≥1 wt %), precipitation occurred once the Pd salt was added to the solution. To obtain a stable solution, the concentration was reduced to 0.1 wt %. At this concentration, the solution remained stable upon reduction of the palladium salt. Here, it is worth noting that the absence of precipitation does not prove the encapsulation of a metal nanoparticle by the individual dendrimer, but confirms the lack of significant dendrimer aggregation. In all further experiments, we used 0.1 wt % dendrimer concentration.

To study the influence of the reduction rate, i.e., nucleation and growth of nanoparticles, we used LiB-

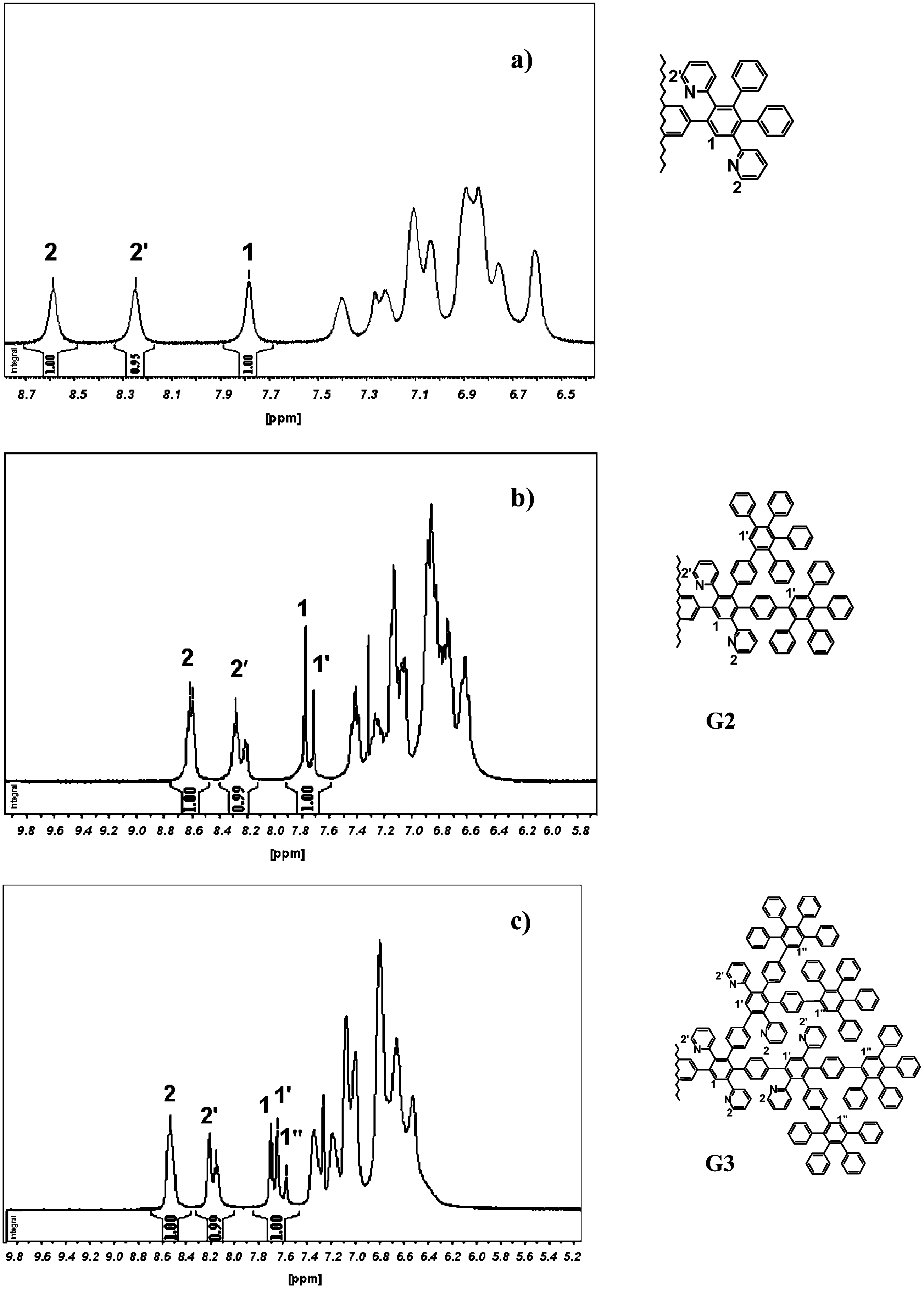

Figure 1. ^{1}H NMR spectra of poly(phenylene-pyridyl) dendrimers of different generations (400 MHz, $CDCl_3$).

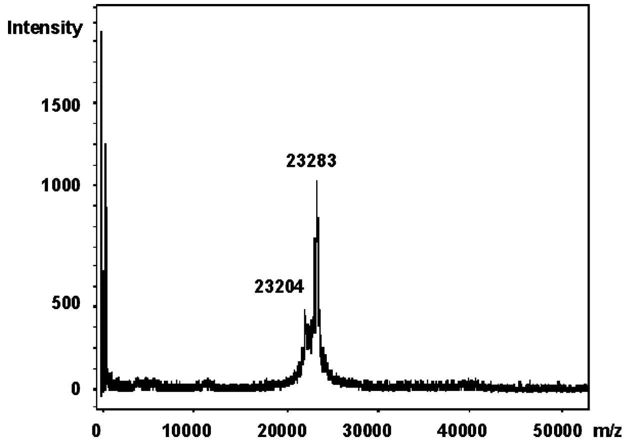

Figure 2. MALDI-TOF spectrum of Td-G4-Ph (**9**) in the presence of potassium ion.

$(C_2H_5)_3H$ as a fast reducing agent[29] and $(C_2H_5)_3SiH$ as a sluggish reducing agent.[30] However, while reduction with $(C_2H_5)_3SiH$ led to the reaction solution that was stable for at least six months, reduction with $LiB(C_2H_5)_3H$ resulted in immediate precipitation. This outcome may sound counterintuitive because, normally, smaller particles produced by fast reduction are more readily stabilized in polymer solutions than larger particles obtained by slow reduction. We assume that, because fast reduction leads to fast nucleation and formation of a large amount of very small Pd nanoparticles, stiff fully aromatic dendrimers are unable to stabilize these particles. Apparently, small nonstabilized particles with high surface energy tend to aggregate and give large metal particles, which cannot be stabilized by dendrimers and precipitate from the solution. This provides evidence that the dendrimer serves as an effective template at a relatively slow reduction rate.

To prove the interaction of the Pd salt with dendrimers, UV–vis spectroscopy was used. Figure 6 depicts the absorption spectra of $Pd(CH_3COO)_2$ in the presence (pink line) and absence (inset) of **9**, the spectrum of encapsulated in **9** Pd nanoparticles (yellow), and the spectrum of **9** (green) vs THF. As evident from the spectra, the interaction of the dendrimer with $Pd(CH_3COO)_2$ causes red-shifted λ_{max} by about 35 nm as compared to the spectrum of pure $Pd(CH_3COO)_2$. This shift corresponds to the ligand-to-metal charge-transfer transition between Pd(II) and pyridine ligands within a dendrimer.[31]

Furthermore, the extinction coefficient (ϵ) for the Pd complex with a dendrimer is higher than that of $Pd(CH_3COO)_2$ by a factor of 1000. These findings indicate that Pd(II) species are coordinated with pyridine nitrogen atoms of a dendrimer. After reduction of the **Td-G4-Ph/Pd(CH$_3$COO)$_2$** complex with $HSi(C_2H_5)_3$, the band observed at 425 nm completely disappeared and a new absorption appeared over a wide wavelength range that is typical of Pd(0) nanoparticles.[32] In addition, the color of the solution changed from yellow to

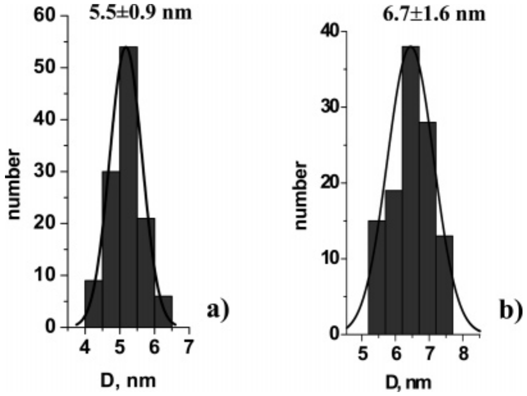

Figure 4. Size distribution of **Td-G3-Ph** (a) and **Td-G4-Ph** (b), derived from AFM data.

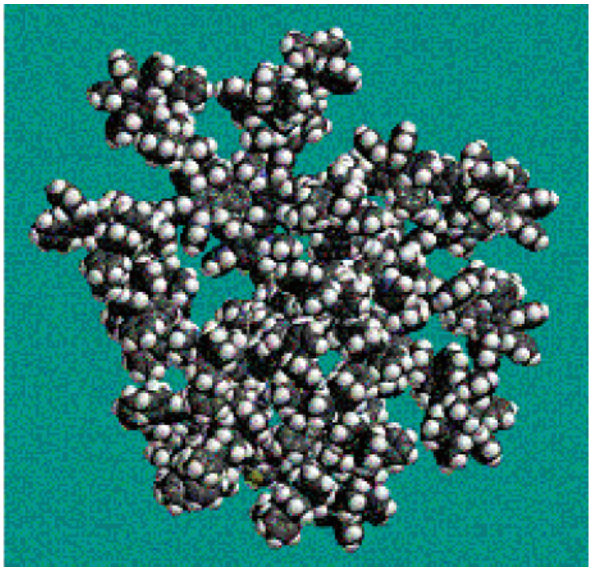

Figure 5. Space-filling view of **Td-G4-Ph** (**9**) dendrimer minimized in energy by molecular dynamics simulation by using FFMM in Spartan software.

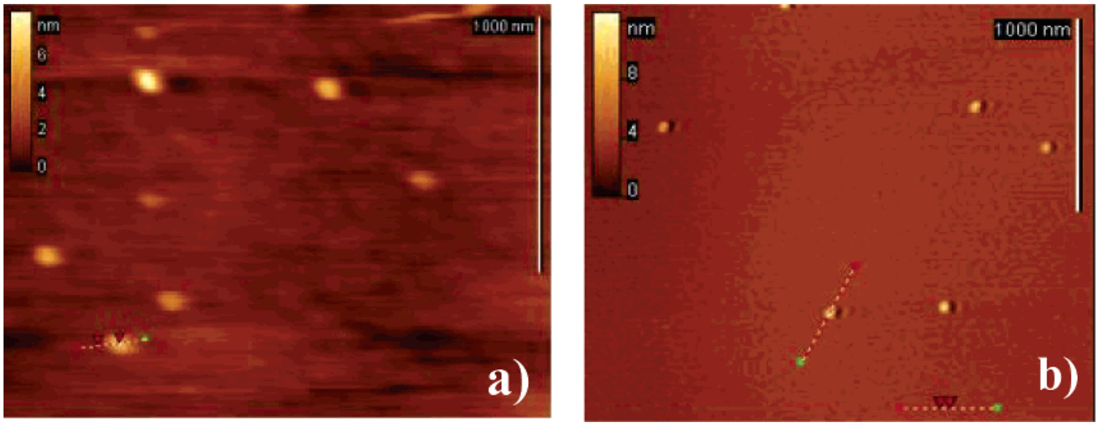

Figure 3. AFM images of **Td-G3-Ph** (a) and **Td-G4-Ph** (b).

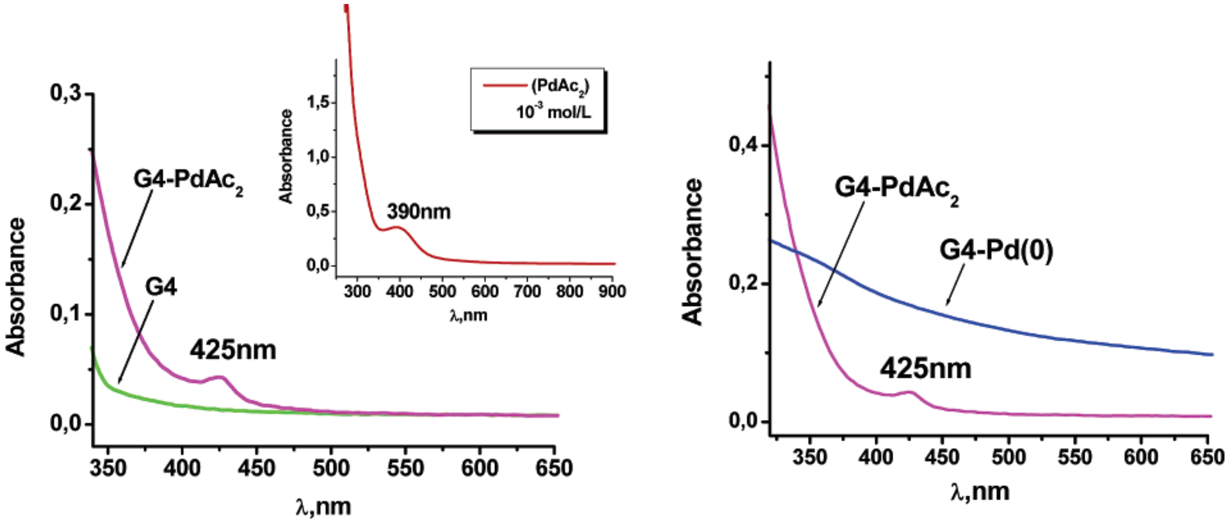

Figure 6. UV−Vis absorption spectra of THF solutions containing **Td-G4-Ph** (**9**) (green), **Td-G4-Ph/Pd(CH_3COO)$_2$** (magenta), **Td-G4-Ph/Pd(0)** (yellow), and Pd(CH_3COO)$_2$ (red inset).

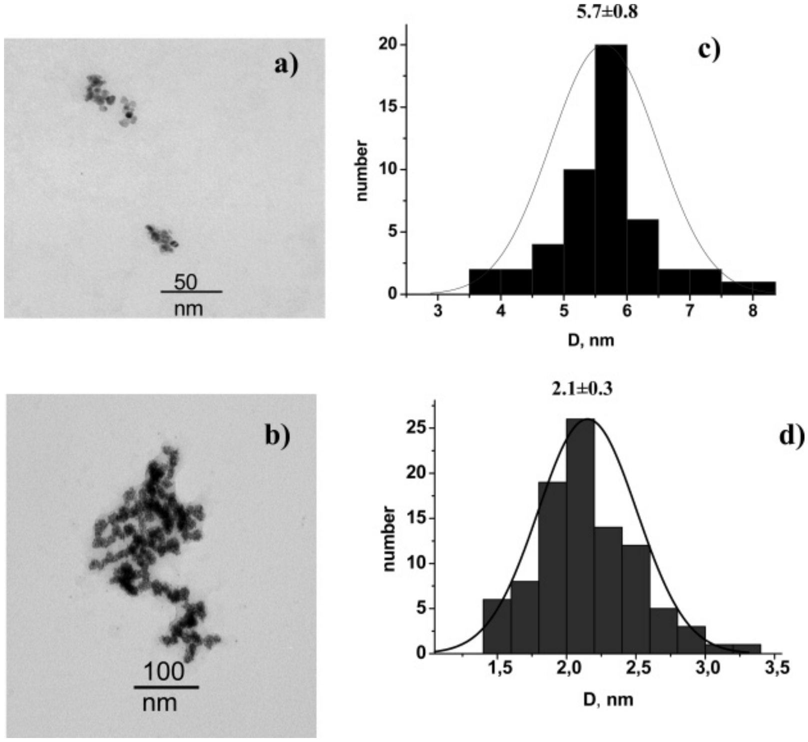

Figure 7. TEM images of **Td-G4-Ph**, containing Pd(II) (a) and Pd(0) (b) and histograms (c) and (d) of size distribution for these samples.

dark brown after reduction. No precipitation was observed for more than six months.

Characterization of Dendrimers with Encapsulated Metal Nanoparticles. To study dendrimers with encapsulated metal nanoparticles, we used TEM, DLS, and XRD. We have found that nonmetalated **Td-G4-Ph** (**9**) cannot be successfully imaged by TEM. In both cases (stained sample and without staining), **9** forms films on the carbon-coated electron grid (even when the sample was cast from a very dilute solution); the structural details of these films could not be discerned. Evidently, owing to the rotational mobility of parts of the molecules around single bonds, the dendrimers have a tendency to entangle themselves. On the other hand, the complex of **Td-G4-Ph** with Pd(CH_3COO)$_2$ can be successfully examined (see Figure 7a) because it displays a lesser tendency to form aggregates. It is noteworthy that the presence of Pd species is equivalent to staining and provides good contrast for the area containing Pd (this area should be close to the full dendrimer size except the polyphenylene periphery).

The average size of this dendrimer complex obtained from the TEM image is 5.7 ± 0.8 nm (calculated out of 102 dendrimers), revealing a good agreement with the data obtained from AFM (for **9** it is 6.7 nm), considering that AFM shows a full dendrimer size while TEM shows only an area stained with Pd. The TEM image of the **Td-G4-Ph/Pd(0)** sample (after metal reduction) presented in Figure 7b shows dark circles, which we believe are Pd(0) nanoparticles, separated by light-grey areas (dendrimers) and combined into large aggregates. The particles are not well-separated from each other, but we could measure their size with image analysis software. These particles are relatively monodisperse and possess

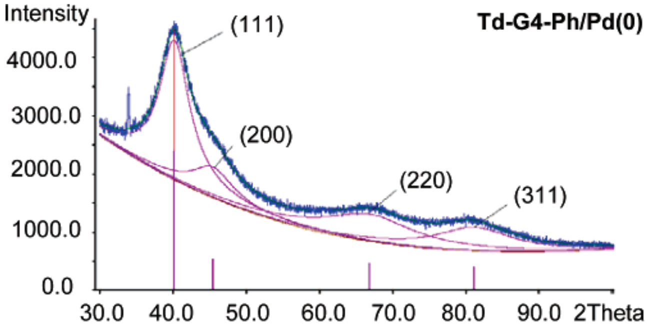

Figure 8. X-ray diffraction profile of **Td-G4-Ph/Pd(0)**.

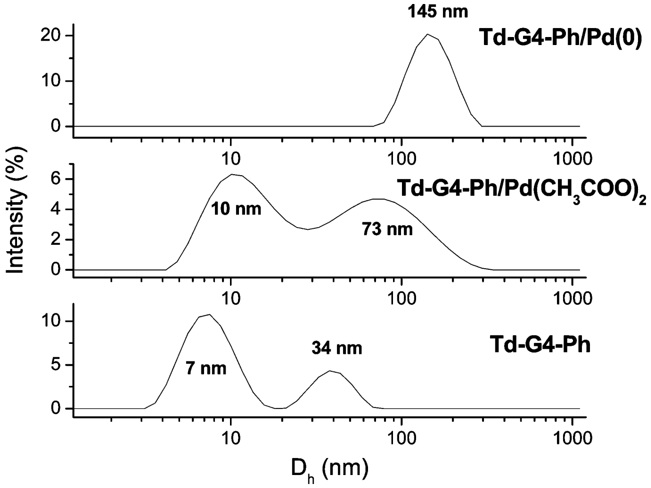

Figure 9. Hydrodynamic diameter distributions of the **Td-G4-Ph** dendrimers before and after metalation at 90° scattering angle and 25 °C in chloroform.

a diameter of 2.1 ± 0.3 nm. This size is larger by a factor of 2 than the expected value of 1 nm calculated for the corresponding dendrimer loading (one palladium per two nitrogens) and confirmed by the elemental analysis. This suggests an exchange between dendrimers leading to larger particles that probably can be better stabilized by these dendrimers.

The XRD pattern of this sample (Figure 8) shows reflexes that are characteristic of Pd crystallites.The average crystallite size is about 2.0 nm, as calculated from the broadening of the (111) reflection by using the Scherrer equation.[33] The XRD pattern also shows an incoherent scattering background coming from the dendrimer matrix.

Figure 9 shows hydrodynamic diameter distributions of the **Td-G4-Ph** (**9**), complex **Td-G4-Ph/Pd(CH_3COO)$_2$**, and **Td-G4-Ph/Pd(0)** in chloroform solutions obtained from DLS measurements. The solution concentration was kept as low as possible to prevent interparticle interaction in solution, namely, 10^{-4} mol/L for **Td-G4-Ph** and 2×10^{-5} mol/L for samples loaded with metal. It appears that **Td-G4-Ph** (**9**) contains two kinds of particles. The major peak at 7 nm is due to dendrimer molecules, while the larger particles are dendrimer aggregates. This value agrees well with the AFM data and calculations (see discussion above). Because the contribution of larger particles to the scattering intensity is much higher than that of smaller particles (the scattering intensity is proportional to the squared volume, i.e., to R^6), the fraction of dendrimer aggregates in chloroform solution is negligible.

Incorporation of palladium acetate into **9** results in the slight increase of the dendrimer hydrodynamic diameter to about 10 nm and an increase of the dendrimer aggregate size, while their fraction remains nearly the same. We suggest that the increase in dendrimer size is due to formation of a solvent shell because of interaction of polar Pd(CH_3COO)$_2$ absorbed by the dendrimer and a THF dipole. This also reveals that the dendrimers loaded with Pd acetate remain intact and aggregates observed on the TEM grid are due to secondary aggregation during sample casting. Conversely, Pd nanoparticle formation results in the formation of large dendrimer aggregates with an average diameter of 145 nm (Figure 9). Apparently, this aggregation exists already in solution and is due to strong interaction between individual dendrimers with encapsulated metal nanoparticles. Despite their sizes, these aggregates are amazingly stable (see discussion above).

Comparison of TEM images of **Td-G3-Ph/Pd(0)** (Figure 10) and **Td-G4-Ph/Pd(0)**, presented in Figure 7b, reveals the nanoparticle formation to be similar in both these dendrimer generations.

Again, in **Td-G3-Ph/Pd(0)**, Pd nanoparticles are much larger (2.3 ± 0.3 nm in diameter) than expected from the dendrimer loading (0.7 nm in diameter), thus revealing extensive exchange of Pd species between dendrimers during nanoparticle formation due to intermolecular collisions. We conclude that small Pd clusters of 0.7 nm cannot be stabilized within stiff aromatic dendrimers, thus exchange between the dendrimers results in larger particles. We also cannot exclude that nanoparticles are stabilized by several **Td-G3-Ph** dendrimer molecules. Such a mechanism of

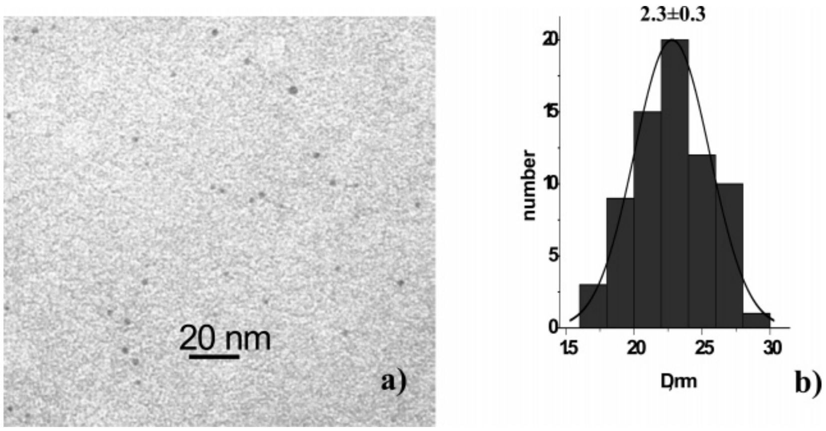

Figure 10. TEM image of Pd(0)-containing **Td-G3-Ph** (a) and histogram of size distribution of Pd nanoparticle diameter (b).

stabilization of metal nanoparticles by low-generation dendrimers was proposed earlier by Gröhn[18] for PAMAM dendrimer and gold nanoparticles. Indeed, the open "starlike" structure of **Td-G3-Ph** supports such a scenario.

For both **Td-G3-Ph/Pd(0)** and **Td-G4-Ph/Pd(0)**, one should expect the existence of the empty dendrimers; however, only for **Td-G3-Ph/Pd(0)** can these empty dendrimers be clearly seen on the TEM grid (as a film on the background). One is led to conclude that, for **Td-G4-Ph/Pd(0)**, the fraction of these dendrimers is smaller and that they are participating in the formation of aggregates in the solution (thus they are not seen on the background). Although these fully aromatic dendrimers loaded with metal nanoparticles form large aggregates in organic solutions, the stability of these solutions and the accessibility of Pd nanoparticles due to the open and rigid dendrimer structure qualifies them as promising catalytic systems for catalytic reactions.

Conclusion and Outlook

A family of stiff polyphenylene dendrimers decorated internally and/or peripherally with pyridine units was synthesized by Diels−Alder cycloaddition by using the divergent method. This approach allowed a robust synthesis of monodisperse dendrimers up to the fourth generation with molecular masses of more than 23 000 g/mol. The solubility of dendrimers was found to depend on the nature of the periphery rather than on the generation. The dendrimers synthesized have outstanding thermal stability similar to that of linear polyphenylenes.

The presence of pyridine moieties in the dendrimers allowed embedding of metal species, namely, Pd acetate. Subsequent reduction of fixed Pd(II) species leads to formation of Pd(0) nanoparticles stabilized by the dendrimer(s). Only polyphenylene-decorated dendrimers with a pyridine−benzene interior were found to obey this scenario, while peripherally, pyridine-decorated molecules precipitated from reaction solutions due to intermolecular coordination with a Pd salt.

TEM, along with DLS, revealed the tendency of dendrimers to form aggregates. For **Td-G4-Ph** and **Td-G4-Ph/Pd$(CH_3COO)_2$**, aggregates were observed only on the TEM grids, while almost no aggregation was found in solutions. Conversely, for **Td-G4-Ph/Pd(0)**, large dendrimer aggregates were observed both in solution (DLS) and on the carbon-coated grid (TEM). At the same time, **Td-G4-Ph/Pd(0)** displays a remarkable solution stability (for more than six months) without any detectable changes. As supported by TEM and XRD, Pd nanoparticles of 2 nm in diameter are encapsulated within dendrimers, revealing that so-called "host−guest nanoscale synthesis" has been achieved for the first time for rigid, completely aromatic dendrimers.

One of the most promising aspects of dendrimer-encapsulated Pd nanoparticles is that they can be used as catalysts in some reactions of interest, e.g., hydrogenation. Herein, the dendrimer fraction of the nanocomposite due to its rigidity and open structure can offer easy access of substrates to catalytic centers, leading to higher catalytic activity. Moreover, the high thermal stability of a dendrimer template will open an opportunity for high-temperature catalytic applications where aliphatic dendrimers and polymers cannot be used. In addition, the periphery of the dendrimers can be configured to attach dendrimers to the alumina or silica surfaces for application in heterogeneous catalysis. While this paper deals with the synthesis of the new dendrimers and the formation and characterization of the dendrimer-encapsulated metal nanoparticles, the application of these materials in catalysis will be presented in a forthcoming article.

Acknowledgment. Financial support from the Alexander von Humboldt Foundation and the Russian Foundation for Basic Research (project 03-03-33017) is gratefully acknowledged.

References and Notes

(1) (a) Tomalia, D. A. *Prog. Polym. Sci.* **2005**, *30*, 294. (b) *Advances in Dendritic Macromolecules*; Newkome, G. R., Ed.; Elsevier Science: Amsterdam, 2002; Vol. 5, p 254. (c) Gitsov, I.; Lin, C. *Curr. Org. Chem.* **2005**, *9*, 1025.

(2) Buhleier, E. W.; Wehner, W.; Vögtle, F. *Synthesis* **1978**, 155.

(3) (a) Denkewalter, R. G.; Kolc, J.; Lukasavage, W. J. U.S. Patent. 4,289,872, September 15, 1981. (b) Denkewalter, R. G.; Kolc, J.; Lukasavage, W. J. U.S. Patent 4,360,646, November 23, 1982. (c) Denkewalter, R. G.; Kolc, J.; Lukasavage, W. J. U.S. Patent 4,410,688, October 18, 1983.

(4) (a) Newkome, G. R.; Moorefield, C.N.; Vögtle, F. *Dendritic Molecules: Concepts, Synthesis, Perspectives*; VCH: Weinheim, 1996. (b) Newkome, G. R.; Moorefield, C.N.; Vögtle, F. *Dendrimers and Dendrons: Concepts, Synthesis, Application*; VCH: Weinheim, 2001.

(5) Smith, D. K.; Diederich, F. *Chem.—Eur. J.* **1998**, *4*, 1353.

(6) Mongin, O.; Gossauer, A. *Tetrahedron Lett.* **1996**, *37*, 3825.

(7) (a) Duncan, R.; Kopecek, J. *Adv. Polym. Sci.* **1984**, *57*, 51. (b) Peppas, N. A.; Nagai, T.; Miyajima, M. *Pharm. Technol. Jpn.* **1994**, *10*, 611.

(8) Twyman, L.; King, A. S. H.; Martin, I. K. *Chem. Soc. Rev.* **2002**, *31*, 69.

(9) Brocorens, P.; Zojer, E.; Cornil, J.; Shuai, Z.; Leising G.; Müllen, K.; Brédas, J. L. *Synth. Met.* **1999**, *100*, 141.

(10) Wiesler, U.-M.; Berresheim, A. J.; Morgenroth, F.; Lieser, G.; Muellen, K. *Macromolecules* **2001**, *34*, 187.

(11) Morgenroth, F.; Reuther, E.; Muellen, K. *Angew. Chem., Int. Ed. Engl.* **1997**, *36*, 631.

(12) (a) Morgenroth, F.; Muellen, K. *Tetrahedron* **1997**, *53*, 15349. (b) Berresheim, A. J.; Morgenroth, F.; Wiesler, U. M.; Muellen, K. *Polymer Prepr.* **1998**, *39* (1), 721. (c) Morgenroth, F.; Kuebel, C.; Muellen, K. *J. Mater. Chem.* **1997**, *7*, 1207. (d) Morgenroth, F.; Kuebel, C; Mueller, M; Berresheim, A. J.; Wiesler, U. M.; Wagner, M.; Muellen, K. *Carbon* **1998**, *36*, 833. (e) Morgenroth, F.; Berresheim, A. J.; Wagner, M.; Muellen, K. *Chem. Commun.* **1998**, 1139.

(13) (a) Miller, T. M.; Neenan, T. X. *Chem. Mater.* **1990**, *2*, 346. (b) Miller, T. M.; Neenan, T. X.; Bair, Y. E. *Polym. Prepr.* **1991**, *32* (3), 627.

(14) Zhao, M.; Sun, L.; Crooks, R. M. *J. Am. Chem. Soc.* **1998**, *120*, 4877.

(15) Balogh, L.; Tomalia, D. A. *J. Am. Chem. Soc.* **1998**, *120*, 7355.

(16) Jansen, J. F. G. A.; de Brabander-van den Berg, E. M. M.; Meijer, E. W. *Science* **1994**, *266*, 1226.

(17) (a) Crooks, R. M.; Zhao M.; Sun. L.; Chechnik, V.; Yeung L. K. *Acc. Chem. Res* **2001**, *34,* 181. (b) Scott, R. W. J.; Wilson, O. M.; Crooks, R. M. *J. Phys. Chem. B* **2005**, *109*, 692.

(18) Gröhn, F.; Bauer, B. J.; Akpalu, Y. A.; Jackson, C. L.; Amis, E. J. *Macromolecules* **2000**, *33*, 6042.

(19) The core was synthesized by Hagihara method via Pd-catalyzed coupling of trimethylsilylethyne with tetrakis(4-iodphenyl)methane, followed by the removing of trimethylsilyl protecting groups. See: Takahashi, S.; Koroyama, Y.; Sonogashira, K.; Hagihara, N. *Synthesis* **1980**, 627; Su, D.; Menger, F. M. *Tetrahedron Lett.* **1997**, *38*, 1485; Simard, M.; Su, D.; Wuest, J. D. *J. Am. Chem. Soc.* **1991**, *113*, 4696.

(20) Wang, X.; Rabbat, P.; O'Shea, P.; Tillyer, R.; Grabowski, E. J. J.; Reider, P. J. *Tetrahedron Lett.* **2000**, *41*, 4335.

(21) Berresheim, A. J.; Mueller, M.; Muellen, K. *Chem. Rev.* **1999**, *99*, 1747.

(22) Antonietti, M.; Wenz, E.; Bronstein, L.; Seregina, M. *Adv. Mater.* **1995**, *7*, 100.

(23) Spatz, J. P.; Roescher, A.; Möller, M. *Adv. Mater.* **1996**, *8*, 337.

(24) Manna, A.; Imae, T.; Aoi, K.; Okada, M.; Yogo, T. *Chem. Mater.* **2001**, *13*, 1674.
(25) Zhao, M.; Crooks, R. M. *Chem. Mater*. **1999**, *11*, 3379.
(26) Molecular model was built by a Merck molecular force field (MMFF) method in Spartan (Wavefunction, Inc., Irvine, CA).
(27) (a) Bronstein, L. M.; Chernyshov, D. M.; Volkov, I. O.; Ezernitskaya, M. G.; Valetsky, P. M.; Matveeva, V. G.; Sulman, E. M. *J. Catal.* **2000**, *196*, 302. (b) Rutnakornpituk, M.; Thompson, M. S.; Harris, L. A.; Farmer, K. E.; Esker, A. R.; Riffle, J. S.; Connolly, J.; St. Pierre, T. G. *Polymer* **2002**, *43*, 2337.
(28) Canty, A. J. In *Comprehensive Organometallic Chemistry II*; Abel, E. W., Stone, F. G. A, Wilkinson, G., Eds.; Elsevier Science: New York, 1995; Vol. 9, p 225.
(29) Seregina, M. V.; Bronstein, L. M.; Platonova, O. A.; Chernyshov, D. M.; Valetsky, P. M.; Hartmann, J.; Wenz, E.; Antonietti, M. *Chem. Mater.* **1997**, *9*, 923.
(30) Sidorov, S. N.; Bronstein, L. M.; Kabachii, Y. A.; Valetsky, P. M.; Soo, P.; Maysinger, D.; Eisenberg, A. *Langmuir* **2004**, *20*, 3543.
(31) Kreibig, U.; Vollmer, M. *Optical Properties of Metal Clusters*; Springer: Berlin, 1995.
(32) Scott., R. W. J.; Ye, H.; Henriquez, R. R.; Crooks, R. M. *Chem. Mater*. **2003**, *15*, 3873.
(33) Warren, B. E. *X-ray Diffraction*; Dover: New York, 1990.

MA051802N